RSC Advances

ROYAL SOCIETY OF CHEMISTRY

www.rsc.org/advances

Cite this: DOI: 10.1039/c0xx00000x

www.rsc.org/xxxxxx

ARTICLE TYPE

Single-walled carbon nanohorns with unique horn-shaped structures as scaffold for lithium-sulfur batteries

Wangliang Wu[a,b,c], Yi Zhao[a,b], Chuxin Wu[a,b], Lunhui Guan[a,b*]

Received (in XXX, XXX) Xth XXXXXXXXX 20XX, Accepted Xth XXXXXXXXX 20XX

DOI: 10.1039/b000000x

A novel single-walled carbon nanohorns-sulfur composite with high sulfur content up to 76% was firstly synthesized via a straightforward melt-infusion strategy. The composite exhibits excellent electrochemical performance with a high capacity of 693 mAh g^{-1} remained after 100 cycles at a high rate of 1.6 A g^{-1}.

With the burgeoning needs of electric vehicles and smart grids, lithium-sulfur (Li-S) batteries are being sought for the next generation rechargeable battery system due to their high theoretical capacity of 1675 mA h g^{-1} and energy density of 2600 Wh kg^{-1}, as well as natural abundance, low cost, and environmental neutrality of elemental sulfur.[1-3] Despite these considerable advantages, Li-S batteries still suffer from problems that prohibit their practical applications. The first challenge is the volume change of sulfur particles during the discharge/charge processes leading to the structural collapse of the cathode and thus fast capacity decay. Second, sulfur is both ionic and electronic insulator, which increases the internal resistances of the batteries leading to a large polarization and thus poor active material utilization. Third, the intermediate discharge products Li_2S_n ($2<n\leq8$) are soluble in organic electrolytes leading to the shuttle effect and thus low coulombic efficiency.[4] One of the most promising approaches to address these issues is to combine sulfur with the conducting carbon matrices such as muti-walled carbon nanotubes (MWCNTs),[5-7] single-walled carbon nanotubes (SWCNTs),[8] and graphene.[9-11] As new carbon materials, single-walled carbon nanohorns (SWCNHs) are composed of thousands of graphitic tubule closed ends with cone-shaped horns. On account of large surface area, high pore volume, good electrical conductivity, and a unique horn-shaped structure, they then have been used as a conductive support for gas storage, catalyst, biomedical applications, supercapacitor, lithium ion batteries, etc.[12-15] Therefore, it is a promising carbon matrix material for the Li-S batteries. Herein, SWCNHs have been explored as scaffold for the Li-S batteries. The sulfur content in the SWCNHs-S composite is up to 76 %, greatly increasing the overall energy density per gram of cathode. The composite exhibited excellent rate capability and cycle stability, even at a high rate of 1.6 A g^{-1}.

The SWCNHs-S composite was prepared via a facile melt-diffusion method as described in Fig. 1a (and see ESI for more details). The morphology and microstructure of the SWCNHs and SWCNHs-S composites were characterized by scanning electron microscope (SEM) and transmission electron microscope (TEM).

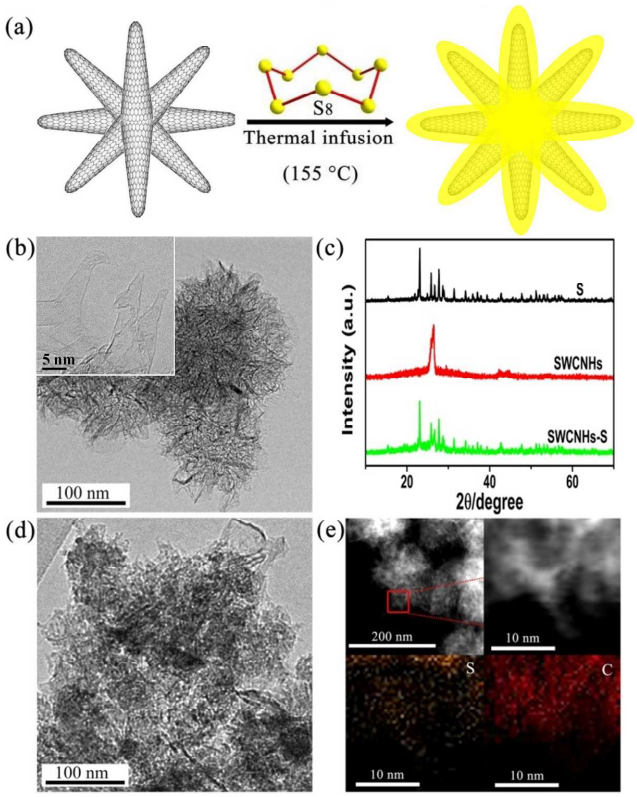

Fig. 1 (a) Schematic illustration of the SWCNHs-S composite; (b) TEM image of the SWCNHs; (c) XRD patterns of the sublimed S, SWCNHs, and SWCNHs-S; (d) TEM image of the SWCNHs-S composite; (e) elemental mapping and elemental analysis results for the SWCNHs-S composite.

As seen in Fig. 1b and Fig. S1, the SWCNHs exhibited dahlia-flower-like spherical aggregates with conical tips, and the particles were approximately 100 nm in size. After incorporation of sulfur, the surface of the SWCNHs was decorated with sulfur particles in Figure 1d. The forks between adjacent horn tips could contribute to effective anchoring of sulfur and trapping of soluble Li_2S_n. Moreover, energy dispersive spectroscopy (EDS) mapping of the composite was carried out to further verify the structure and composite of the SWCNHs-S in Fig. 1e and Fig. S4. The corresponding element mapping of S and C showed that S was indeed dispersed into the pores and on the surface of SWCNHs. This was consistent with the XRD analysis result in Fig. 1c. All

the original diffraction peaks of crystalline S were retained in the SWCNHs-S composite. However, a characteristic peak at around 26° of the SWCNHs was not clearly observed in the SWCNHs-S composite. The thermal analysis result determined that the S content was 76% for the SWCNHs-S composite in Fig. S2.

Nitrogen adsorption–desorption isotherms were used to investigate the porous structures of the SWCNHs and SWCNHs-S in Fig. 2a. The SWCNHs exhibited mixed type I and II isotherms, indicating the existence of a pore size range from micropores to macropores.[16] However, the SWCNHs-S composite showed almost zero adsorption at the micropore region, demonstrating that these micropores were filled with S. In addition, a depletion of the hysteresis loop was found in the composite, also indicating the mesopores were filled. As can be seen in Table 1 (see ESI), the SWCNHs had a large Brunauer-Emmett-Teller (BET) surface area of 203 m^2 g^{-1} and a high pore volume of 0.48 cm^3 g^{-1}, which could be benefit to retain polysulfides from dissolving into the electrolyte and thus improve the cycle stability due to a strong adsorption of the pores structure for the active material and the soluble polysulphides. Whereas, the BET surface area and the pore volume of SWCNHs-S dramatically decreased to 0.94 m^2 g^{-1} and 0.01 cm^3 g^{-1}, respectively. The tremendous changes in the surface area and porosity of the samples reconfirmed that S was indeed dispersed into the pores and on the surface of SWCNHs. The porous structure of the SWCNHs could be further determined by the pore size distribution curves in Fig. 2b. The pore sizes of the SWCNHs were mainly centred at 0.7, 2.2, 3.8, and 22 nm.

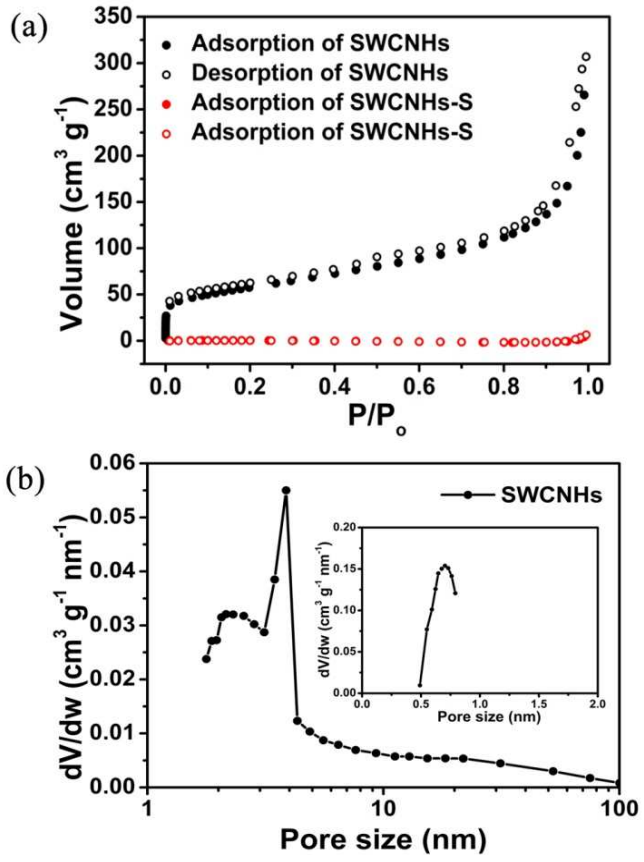

Fig. 2 (a) N_2 adsorption–desorption isotherms of the SWCNHs and SWCNHs-S; (b) pore size distribution curves of SWCNHs.

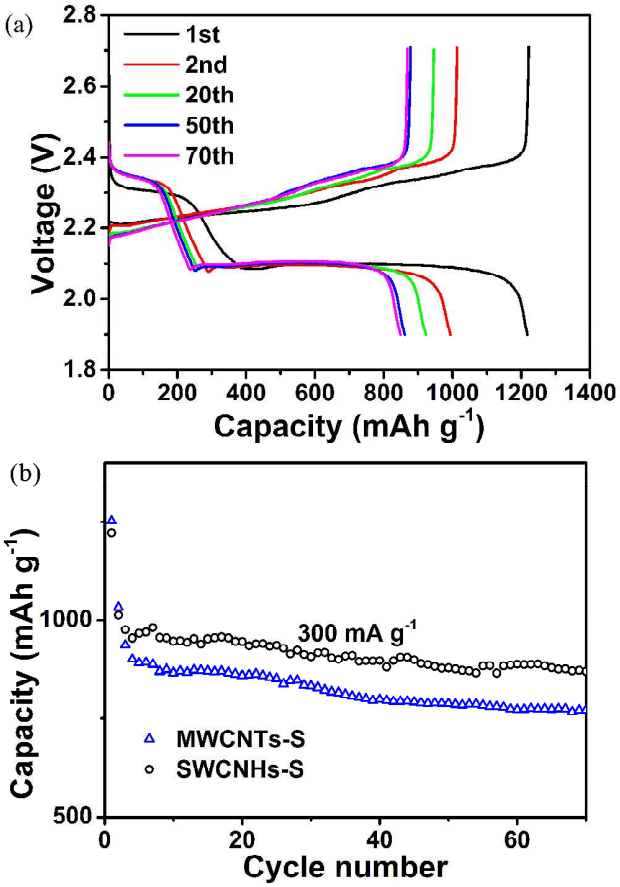

Fig. 3 (a) Typical voltage capacity profiles of SWCNHs-S; (b) cycle stability of SWCNHs-S and MWCNTs-S at 300 mA g^{-1}.

The voltage capacity profiles of SWCNHs-S composite were exhibited in Fig. 3a. The curves demonstrated two typical discharge plateaus and two closely spaced charge plateaus, which were consistent with the cyclic voltammogram plots in Fig. S3. The upper discharge plateau at around 2.3 V represented the transformation of sulphur into long-chain polysulphides (Li_2S_n; where n is typically 4–8) and the lower discharge plateau at about 2.1 V represented the conversion of short-chain polysulphides (Li_2S_2/Li_2S), which were reminiscent in the charge plateaus as well.[17, 18] Moreover, the second discharge plateau was very flat, revealing a uniform deposition of Li_2S with little kinetic barriers.[19, 20] The cycling performance of the SWCNHs-S composite was shown in Fig. 3b. An initial discharge specific capacity of the SWCNHs-S composite was 1218 mA h g^{-1} and retained a reversible capacity of 849 mA h g^{-1} after 70 cycles at 300 mA g^{-1}. In contrast, the electrode made of MWCNTs-S composite only remained at 761 mA h g^{-1}. The good cycling stability was attributed to the large electrochemically active surface area of the SWCNHs, which provided the intimate contact with S to suppress the dissolution of the polysulphides and a short transport pathway for both electrons and Li^+. Compared with MWNTs, the unique structure properties of SWCNHs resulted in larger surface area, which could effectively hamper the dissolution of lithium polysulfides during discharge/charge cycles, thus to achieve the high specific capacity and good cycling retention.

Fig. 4a shows that the SWCNHs-S composite delivered a

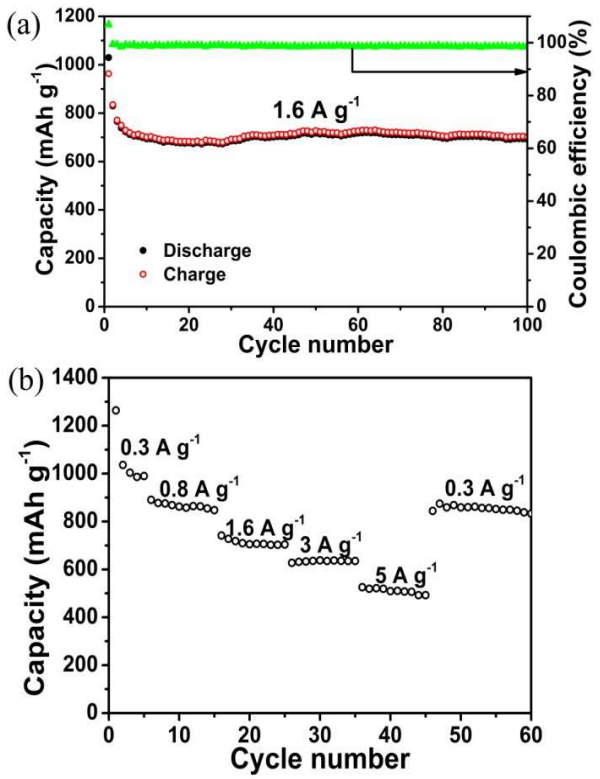

Fig. 4 (a) cycle performance and coulombic efficiency of the SWCNHs-S composite at a high current density of 1.6 A g-1; (b) rate capability of the SWCNHs-S composite.

specific capacity of 1030 mA h g^{-1} and still maintained at 693 mA h g^{-1} after 100 cycles at a high rate of 1.6 A g^{-1}, representing good cycle stability. Furthermore, the average coulombic efficiency of the composite was approximately 99%, indicating a high activematerial utilization. The rate capability of the SWCNHs-S composite was carried out at various rates in Fig. 4b. The composite delivered a capacity of around 1000 mA h g^{-1} after five cycles at 0.3 A g^{-1}. Even at a high rate of 5 A g^{-1}, the composite also revealed a high capacity of 500 mA h g^{-1}. When the rate was returned to 0.3 A g^{-1}, the discharge capacity can be mostly recovered at 833 mA h g^{-1} after 60 cycles. The excellent electrochemical performance can be understood through the following reasons: First, the forks between adjacent horn tips of the SWCNHs could be served as a scaffold for intimate interactions with S to anchor the active materials. This intimate interaction was avail to the fast transport of electrons and lithium ions. Second, the high surface area of SWCNHs were beneficial for the adsorption of S and polysulfides and thus improving the electrochemical performance. Third, the high conductivity of new carbon materials was helpful in overcoming the electrical insulation of S to improve the active materials utilization.

Conclusions

In summary, a novel SWCNHs-S composite with high S content up to 76% was successfully prepared by a facile melt-infusion method. Due to the unique horn-shaped structure of SWCNHs with high surface area, the SWCNHs-S composite delivered a capacity of 1218 mA h g^{-1}, and retained at 849 mA h g^{-1} after 70 cycles at 300 mA g^{-1}. Even at a high rate of 1.6 A g^{-1}, the initial capacity of 1030 mA h g^{-1} was achieved and it maintained at 693 mA h g^{-1} after 100 cycles. Hence, the composite exhibited the excellent rate capability and cycle stability, which made the SWCNHs to be a promising porous carbon matrix material for enhancing the performance of the Li-S batteries.

We acknowledge the financial support provided by the National Key Project on Basic Research (Grant no. 2011CB935904), the National Natural Science Foundation of China (Grant no. 21171163, 91127020) and NSF for Distinguished Young Scholars of Fujian Province (Grant no. 2013J06006).

Notes and references

[a] *State Key Laboratory of Structural Chemistry, Fujian Institute of Research on the Structure of Matter, Chinese Academy of Sciences, YangQiao West Road 155#, Fuzhou, Fujian, P. R. China. Fax: +86-591-83792835; Tel: +86-591-83792835; E-mail: guanlh@fjirsm.ac.cn*
[b] *Key Laboratory of Design and Assembly of Functional Nanostructures, Chinese Academy of Sciences, Fuzhou, Fujian 350002, China*
[c] *Graduate University of Chinese Academy of Sciences, Beijing, P. R. China*

† Electronic Supplementary Information (ESI) available: [Experimental section, SEM, TGA, CV and EIS measurements]. See DOI: 10.1039/b000000x/

1. B. Dunn, H. Kamath and J. M. Tarascon, *Science*, 2011, 334, 928-935.
2. X. Ji, K. T. Lee and L. F. Nazar, *Nat. Mater.*, 2009, 8, 500-506.
3. Y. X. Yin, S. Xin, Y. G. Guo and L. J. Wan, *Angew. Chem., Int. Ed.*, 2013, 52, 13186-13200.
4. Y. Yang, G. Zheng and Y. Cui, *Chem. Soc. Rev.*, 2013, 42, 3018-3032.
5. L. Yuan, H. Yuan, X. Qiu, L. Chen and W. Zhu, *J. Power Sources*, 2009, 189, 1141-1146.
6. S. Xin, L. Gu, N. H. Zhao, Y. X. Yin, L. J. Zhou, Y. G. Guo and L. J. Wan, *J. Am. Chem. Soc.*, 2012, 134, 18510-18513.
7. C. Wang, H. Chen, W. Dong, J. Ge, W. Lu, X. Wu, L. Guo and L. Chen, *Chem. Commun.* , 2014, 50, 1202-1204.
8. S. M. Zhang, Q. Zhang, J. Q. Huang, X. F. Liu, W. Zhu, M. Q. Zhao, W. Z. Qian and F. Wei, *Part. Part. Syst. Charact.*, 2013, 30, 158-165.
9. J. Z. Wang, L. Lu, M. Choucair, J. A. Stride, X. Xu and H. K. Liu, *J. Power Sources*, 2011, 196, 7030-7034.
10. G. Zhou, S. Pei, L. Li, D. W. Wang, S. Wang, K. Huang, L. C. Yin, F. Li and H. M. Cheng, *Adv. Mater.*, 2013, 26, 625–631.
11. J. Rong, M. Ge, X. Fang and C. Zhou, *Nano Lett.*, 2013, *14* (2), 473-479.
12. S. Zhu and G. Xu, *Nanoscale*, 2010, 2, 2538-2549.
13. H. J. Jung, Y. J. Kim, J. H. Han, M. Yudasaka, S. Iijima, H. Kanoh, Y. A. Kim, K. Kaneko and C. M. Yang, *J. Phys. Chem. C*, 2013, 117, 25877-25883.
14. Y. Zhao, J. Li, Y. Ding and L. Guan, *Chem. Commun.*, 2011, 47, 7416-7418.
15. Y. Liu, C. M. Brown, D. A. Neumann, D. B. Geohegan, A. A. Puretzky, C. M. Rouleau, H. Hu, D. Styers Barnett, P. O. Krasnov and B. I. Yakobson, *Carbon*, 2012, 50, 4953-4964.
16. Y. S. Su and A. Manthiram, *Nat. Commun.*, 2012, 3, 1166.
17. H. Yamin, A. Gorenshtein, J. Penciner, Y. Sternberg and E. Peled, *J. Electrochem. Soc.*, 1988, 1045-1048.
18. W. Zhou, Y. Yu, H. Chen, F. J. DiSalvo and H. D. Abruna, *J. Am. Chem. Soc.*, 2013, 135, 16736-16743.
19. G. Zheng, Y. Yang, J. J. Cha, S. S. Hong and Y. Cui, *Nano Lett.*, 2011, 11, 4462-4467.
20. T. Lin, Y. Tang, Y. Wang, H. Bi, Z. Liu, F. Huang, X. Xie and M. Jiang, *Energy Environ. Sci.*, 2013, 6, 1283.

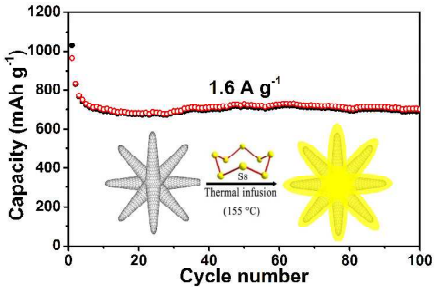

A new SWCNHs-S composite exhibited excellent cycle stability with 693 mAh g^{-1} remained after 100 cycles at 1600 mA g^{-1}.